

"Rapid Prototyping" of Biosensing Surface Plasmon Resonance Devices using COMSOL & Matlab Software

Dominic Carrier and Jan J. Dubowski

Department of Electrical and Computer Engineering, Université de Sherbrooke
Sherbrooke, Québec, J1K 2R1, Canada, E-mail: dominic.carrier@usherbrooke.ca

Abstract: We present a Finite Element Method simulation procedure that allows rapid development of prototype devices comprising novel self-referenced interference SPR (surface plasmon resonance) biosensing microstructures. The procedure takes advantage of commercial Comsol Multiphysics and Matlab software and their bi-directional link.

Keywords: Biosensor, surface plasmon resonance, FEM, Comsol, phase measurement.

1. Introduction

Numerous papers presenting results of research on surface plasmon resonance (SPR) effect for biosensing use commercial apparatus [1, 2]. The focus of our research is to provide a new scheme of biosensing with increased sensitivity and specificity, or to offer other advantages, such as a possibility of integration. To allow this latitude of research, exploration of flexible biosensing geometry must be possible. Computer simulation offers this kind of latitude, albeit also presenting some difficulties of its own [3].

Many approaches have already been applied to model physical effects and carry out computer simulations in plasmonics and photonics. Green's tensor approach [4-6], scattering-matrix formalism [7-9] and FEM simulations [10-12] are common methods employed. Green's tensor and scattering matrix methods are restricted to specific modeling scheme (regular "analytic" background and layered architecture respectively [8, 13-15]) whereas Finite Element Method (FEM) does not present such restrictions. The FEM approach is arguably the most user-friendly computing interface. With commercially available FEM software, designing new models, simulation and visualization of the results has become an increasingly common path of advanced research. Generally, the FEM approach is less convenient in terms of computational power required and the raw form of results or, sometimes, accuracy, but it presents

flexibility attractive for undertaking new research.

1.1 SPR biosensing

Diverse fundamental methods were and are currently under investigation to create biosensing devices. Surface acoustic waves, micro-cantilevers, surface plasmon resonance and optical mode probing are only common example avenues of development [16-21]. Commercial SPR systems have been available for more than 15 years [22] and methods have been developed to make measurement of the same fundamental phenomenon more sensitive over the years [23-25]. Combining SPR with phase interference measurement yet still preserving integrability and ease-of-measurement is our goal in the development of a biosensing device.

2. "Rapid-prototyping" methodology for simulation

The availability of commercial software to produce FEM simulations has tremendously accelerated the problem-solving process; the solving engine is already built and verified, the user interface (UI) provides CAD tools to design with, and the software generally comes with examples, tutorials and documentation to help users transfer their problem to the simulation environment. Our research makes use of Comsol Multiphysics software and its close integration with Matlab. The close integration of a high-level programming environment with the strengths and ease-of-use of a mature UI was invaluable to our research, as flexibility of design (use of templates) and advanced parameterization were significant to efficiently achieve these results.

2.1 Modularity

Rapid development of simulation models has been achieved with a programming paradigm, i.e., modularity [26]. When designing complex

systems, separating the different composing elements into smaller and simpler building blocks presents many advantages [27]; those that concern our applications are adaptability and reusability. Segmenting the model creation into its building block elements concedes a considerable flexibility of the final models and reduces considerably models' construction time. It must be noted though that the advantage of modularity emerges when multiple models are to be built or a single model is to be repeatedly and heavily modified; additionally, only the elements that would be reused or adapted can be made modular, thus allowing the required flexibility without the overhead of a complete transformation.

3. Case Study - Self-referenced Biosensor

Surface plasmon modes are a specific solution to Maxwell's equations, viable in the context of a metal-dielectric interface. As such, they present the same characteristics as optical modes, such as reflections, interferences, scattering and so on [28-31]. Using these properties, the proposed biosensor acts as a self-referenced interferometer. The optical path length difference is measured with two coherent surface plasmons, by observing the resultant constructive or destructive interference.

3.1 Model

A coherent light source is directed at the biosensor at normal incidence and is coupled to surface plasmons through the first diffraction order of the "bounding gratings". Each grating will emit surface plasmon modes propagating in opposite directions. Of these two modes, one will go through the sensing surface (delimited by the area between the two bounding gratings) and through the second grating, thus interfering with its "neighbor plasmon". A change of refractive index within the sensing area will induce a change of optical path length of one surface plasmon, thus modulating the output signal. Figure 1 shows both the conceptual representation of the biosensor and the simulation schematic. The modulation response can be measured with conventional means using scanning near-optical microscopy (SNOM), by scattering or diffracting plasmons on surface

corrugation or even volume scatterers, or by using leakage radiation microscopy (LRM) [32].

The simulation is made using Comsol RF Module, 2D harmonic propagation transverse magnetic (TM) in-plane wave application mode. The FEM model displays a symmetry axis delimiting the center of the sensing area, modeled as a perfect electric conductor (PEC) boundary condition.

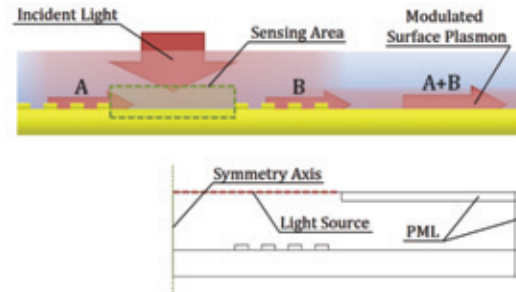


Figure 1 - Proposed biosensor architecture. The upper schematic illustrates the conceptual process of self-referenced interference of surface plasmons. The lower schematic illustrates the simulations details.

A semi-infinite metal-dielectric interface is modeled with incident light coming from the top. The grating periodicity matches the surface plasmon wave-vector for incident energy and angle (0 degree in our case). Refractive indices are taken from experimental data in literature [33, 34]. The perfectly matched layer (PML) regions absorb scattered light and residual surface plasmons. Intensity measurements are made with a boundary integration of the norm of the Poynting vector, thus obtaining a measure of power flowing through that boundary. Perturbation emulation is made with a zone of higher refractive index within the sensing area. To minimize reflections, this perturbation is done by gradually increasing the refractive index instead of having a step function.

3.2 Results

As predicted, we observe a sensible modulation of the propagating plasmon intensity outside the cavity area, which is a function of the refractive index within the sensing area. Figure 2 shows the general shape of the norm of the TM field against the change of refractive index. Clearly observable is the exponential decay

function of the distance and the modulation in amplitude function of the refractive index.

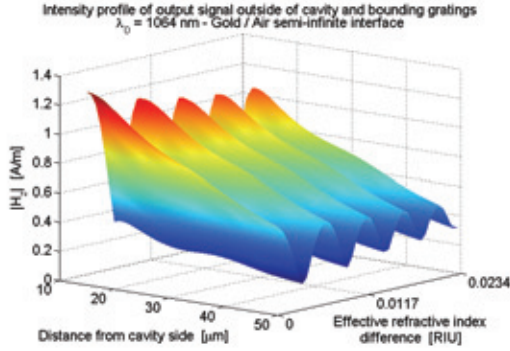


Figure 2 - Shape of the norm of the magnetic field outside the sensing area and bounding gratings, plotted against the effective refractive index within the cavity.

Figure 3 shows the evolution of power flow against the change of refractive index; on the same graph, intensity is normalized following equation [1], in order to emphasize quality of interference.

$$y = \frac{x - x_{min}}{x_{max} + x_{min}} \quad [1]$$

Two characteristic cases were selected to illustrate the cyclic modulation of amplitude of the output mode; this is a direct consequence of the optical path length of the sensing plasmon increasing to more than a full surface plasmon wavelength compared to the reference plasmons, thus going back and forth between constructive and destructive interference mode.

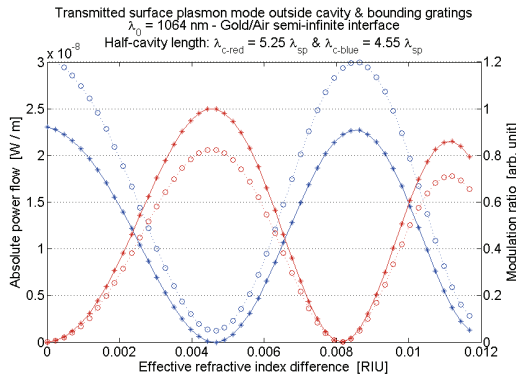


Figure 3 - Modulation of sensor power output from perturbation of the sensing area. Blue and red curve show respectively the modulation based on

constructive and destructive unperturbed state. Circle and stars represents respectively the absolute and normalized scales.

The general behavior and concept is demonstrated clearly with the results summarized in Figure 3. The next step was to investigate the influence of structural parameters on the modulation output. The two investigated parameters are the cavity half-length (the distance from the symmetry axis to the grating) and the length of the grating. Both lengths are normalized to the surface plasmon wavelength (the normalized grating length is equivalent to the number of periods).

Each simulation scanned the same range of refractive indices (as illustrated in figure 3) and the maximum amplitude shift was extracted from each of these sweep (largest modulation), as well as maximum quality factor of interference (see eq.[1]). Figures 4 and 5 (next page) show the evolution of modulation amplitude as a function of the normalized cavity length and normalized grating length, respectively.

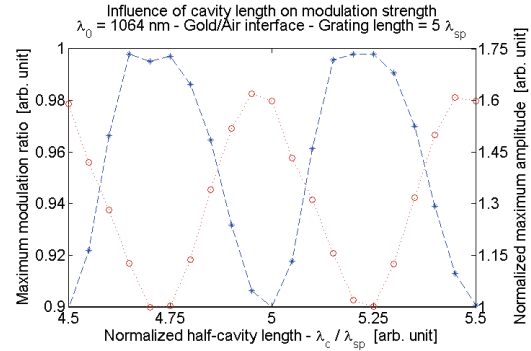


Figure 4 - Influence of cavity length on quality factor of interference and maximum intensity of interference (blue and red curve respectively).

The influence of the cavity length on the output signal is undeniable. The foremost observable strong relation is linked to the initial state of the sensor (constructive or destructive interference when the sensor is unperturbed). When the cavity length (twice the cavity half-length) is an integer, the initial state is constructive; surface plasmons emitted from the gratings are completely in phase. However, when the cavity length is a half-integer (e.g. 9.5, 10.5, etc), the initial state is destructive, as surface plasmons emitted from the gratings are phase

mismatched by half-wavelength. This behavior is still under investigation.

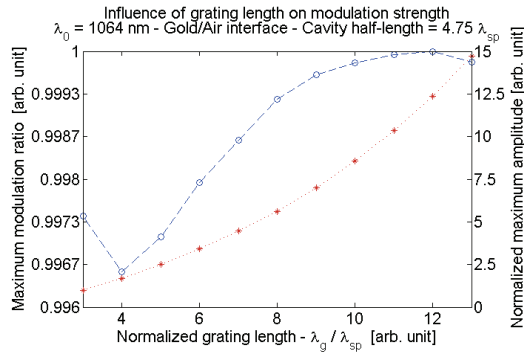


Figure 5 - Influence of grating length on quality factor of interference and maximum intensity of interference (blue and red curve respectively).

When grating length increases, we observe a strong enhancement of the output signal strength, as predicted by coupling theory. Observed values of the quality factor are close to unity, but variations are too small to make conclusions on them for this specific graph (see discussion).

3.3 Discussion

As demonstrated in Fig. 3, the biosensor power output shows a strong modulation induced by relatively small changes of the refractive index. A final sensitivity evaluation is difficult to produce, as it would be much dependent on the measurement method; further investigation are planned to implement the measurement process to the simulations. Although absolute value cannot be assessed, qualitative evaluation of the system is still possible.

We first observe a definite trend of reduction of modulation as the effective refractive index increases (more obvious on a larger sweep that is not presented here). This trend is caused by perturbation of the plasmon mode. A higher refractive index within the sensing area will cause more scattering of the plasmon going through it. The perturbation was defined in such a way as to minimize reflections and scattering, but residual scattering is inevitable, reducing the intensity of the transmitted plasmon. Consequence of this irregular refractive index, the effective optical mode will localize within the perturbation and thus be more absorbed than in the unperturbed case, therefore also reducing

the transmitted plasmon intensity. With this plasmon lower intensity compared to that of the reference plasmon, a partial interference occurs, thus the smaller modulation amplitude.

This phenomenon will reduce the quality of interference as the refractive index increases. Measurements made with smaller refractive indices, thus closer to the unperturbed state, will benefit from greater modulations, therefore achieving better output.

Notice that other factors can enhance or reduce the modulation intensity. We observe a definite relation between size of the sensing area and length of the gratings against propagation length of the plasmons. As the surface plasmon exponentially decays, longer propagation lengths between the sensing and reference plasmon will increase their difference in amplitude, thus reducing the interference amplitude. Figures 4 and 5 do not show this effect as propagation length of surface plasmons at 1.165 eV (free space wavelength of 1064 nm) is well over the lengths investigated here. Thus, for biosensing purpose, lower energies should be employed (such as near infrared for a gold-based interface).

It is suspected that coupling efficiency of the gratings versus the coupling direction (normal incidence to surface mode versus the opposite) is also a factor in the modulation amplitude, since the sensing plasmon has to traverse a complete grating; diffraction on the grating would reduce intensity of the transmitted mode (0th order), thus reducing modulation amplitude. Producing a grating shape that optimizes the efficiency of coupling to surface plasmon versus coupling from surface plasmon would definitely increase this sensor sensitivity, more so if longer gratings were used for intensity purpose.

4. Conclusions

We presented within this article a new approach to FEM modeling, leading to an increased productivity in simulation design by using modular concepts from programming techniques. This method allows greater flexibility and rapidity in simulation creation and exploration, thus making FEM modeling a useful tool for exploratory research prior to experimentation. Using this method, a model of biosensor was created and investigated theoretically. This model presents a novel approach to produce self-referenced phase

measurement of surface plasmon resonance. To be efficient, such a sensor should be employed in the infrared region for a gold substrate, with optimization of grating lengths to sustain maximum modulation amplitude. More research is required to produce quantitative results by integrating the "measurement process" to the simulation.

5. References

1. Rich, R.L. and D.G. Myszka, *Survey of the year 2006 commercial optical biosensor literature*. Journal of Molecular Recognition, 2007. **20**(5): p. 300-366.
2. Rich, R.L. and D.G. Myszka, *Survey of the year 2007 commercial optical biosensor literature*. Journal of Molecular Recognition, 2008. **21**(6): p. 355-400.
3. Jin, J., *Finite Element Method in Electromagnetics, Second Edition*. 2002: John Wiley. 753.
4. Fischer, H. and O.J.F. Martin, *Engineering the optical response of plasmonic nanoantennas*. Opt. Express, 2008. **16**(12): p. 9144-9154.
5. Huang, L., S.J. Maerkl, and O.J. Martin, *Integration of plasmonic trapping in a microfluidic environment*. Opt. Express, 2009. **17**(8): p. 6018-6024.
6. Kottmann, J.P., et al., *Plasmon resonances of silver nanowires with a nonregular cross section*. Physical Review B, 2001. **64**(23): p. 235402.
7. Christ, A., et al., *Symmetry Breaking in a Plasmonic Metamaterial at Optical Wavelength*. Nano Letters, 2008. **8**(8): p. 2171-2175.
8. Lepage, D. and J.J. Dubowski, *Surface plasmon effects induced by uncollimated emission of semiconductor microstructures*. Opt. Express, 2009. **17**(12): p. 10411-10418.
9. Tikhodeev, S.G., et al., *Quasiguidded modes and optical properties of photonic crystal slabs*. Physical Review B, 2002. **66**(4): p. 045102.
10. Dintinger, J. and O.J.F. Martin, *Channel and wedge plasmon modes of metallic V-grooves with finite metal thickness*. Opt. Express, 2009. **17**(4): p. 2364-2374.
11. Dionne, J.A., et al., *PlasMOStor: A Metal-Oxide-Si Field Effect Plasmonic Modulator*. Nano Letters, 2009. **9**(2): p. 897-902.
12. Dionne, J.A., et al., *Are negative index materials achievable with surface plasmon waveguides? A case study of three plasmonic geometries*. Opt. Express, 2008. **16**(23): p. 19001-19017.
13. Martin, O.J.F. and N.B. Piller, *Electromagnetic scattering in polarizable backgrounds*. Physical Review E, 1998. **58**(3): p. 3909.
14. Paulus, M., P. Gay-Balmaz, and O.J.F. Martin, *Accurate and efficient computation of the Green's tensor for stratified media*. Physical Review E, 2000. **62**(4): p. 5797.
15. Paulus, M. and O.J.F. Martin, *Light propagation and scattering in stratified media: a Green's tensor approach*. J. Opt. Soc. Am. A, 2001. **18**(4): p. 854-861.
16. Armani, A.M., et al., *Label-Free, Single-Molecule Detection with Optical Microcavities*. Science, 2007. **317**(5839): p. 783-787.
17. Barbillon, G., et al., *How nanoparticles encapsulating fluorophores allow a double detection of biomolecules by localized surface plasmon resonance and luminescence*. Nanotechnology, 2008. **19**(3): p. 035705.
18. Boriskina, S.V. and L. Dal Negro, *Sensitive label-free biosensing using critical modes in aperiodic photonic structures*. Opt. Express, 2008. **16**(17): p. 12511-12522.
19. Caruso, F., et al., *Quartz Crystal Microbalance Study of DNA Immobilization and Hybridization for Nucleic Acid Sensor Development*. Analytical Chemistry, 1997. **69**(11): p. 2043-2049.
20. Hunt, W.D., et al., *Clues from digital radio regarding biomolecular recognition*. IEEE Transactions on Biomedical Circuits and Systems, 2007. **1**(1): p. 50-5.
21. McKendry, R., et al., *Multiple label-free biodetection and quantitative DNA-binding assays on a nanomechanical cantilever array*. Proceedings of the National Academy of Sciences of the United States of America, 2002. **99**(15): p. 9783-9788.
22. <http://www.biacore.com/lifesciences/history/index.html>.
23. Nemova, G., A.V. Kabashin, and R. Kashyap, *Surface plasmon-polariton Mach-Zehnder refractive index sensor*. J. Opt. Soc. Am. B, 2008. **25**(10): p. 1673-1677.
24. Patskovsky, S., et al., *Mechanical modulation method for ultrasensitive phase measurements in photonics biosensing*. Opt. Express, 2008. **16**(26): p. 21305-21314.
25. Yuan, W., et al., *Surface Plasmon Resonance Biosensor Incorporated in a Michelson*

Interferometer With<newline/>Enhanced Sensitivity. Sensors Journal, IEEE, 2007. **7**(1): p. 70-73.

26. http://en.wikipedia.org/wiki/Programming_paradigm.

27. Meyer, B., *Object-oriented software construction (2nd ed.)*. 1997: Prentice-Hall, Inc. 1254.

28. Barnes, W.L., A. Dereux, and T.W. Ebbesen, *Surface plasmon subwavelength optics*. Nature, 2003. **424**(6950): p. 824-830.

29. Drezet, A., et al., *Surface plasmon interference fringes in back-reflection*. EPL (Europhysics Letters), 2006(4): p. 693.

30. Hecht, B., et al., *Local Excitation, Scattering, and Interference of Surface Plasmons*. Physical Review Letters, 1996. **77**(9): p. 1889.

31. Raether, H., *Surface Plasmons on Smooth and Rough Surfaces and on Gratings (Springer Tracts in Modern Physics)*. 1988: Springer.

32. Drezet, A., et al., *Leakage radiation microscopy of surface plasmon polaritons*. Materials Science and Engineering: B, 2008. **149**(3): p. 220-229.

33. Palik, E.D., *Handbook of optical constants of solids*. 1985, Orlando: Academic Press.

34. Thèye, M.-L., *Investigation of the Optical Properties of Au by Means of Thin Semitransparent Films*. Physical Review B, 1970. **2**(8): p. 3060.

6. Acknowledgements

This work was financed by the Canada Research Chair in Quantum Semiconductors Program.